C. R. Mecanique 343 (2015) 107–120

Contents lists available at ScienceDirect

Comptes Rendus Mecanique

www.sciencedirect.com

Mechanics of granular and polycrystalline solids

Correlation between strength differential effects in the plastic flow of the matrix and the rate of damage growth in porous polycrystals

José Luis Alves [a,b], Oana Cazacu [b,*]

[a] CT2M, Department of Mechanical Engineering, University of Minho, Portugal
[b] Department of Mechanical and Aerospace Engineering, University of Florida, REEF, 1350 N. Poquito Rd., Shalimar, FL 32579, USA

ARTICLE INFO

Article history:
Received 14 January 2014
Accepted 26 April 2014
Available online 7 January 2015

Keywords:
Strength differential effects
Third invariant of stress deviator
Porous polycrystals
Porosity evolution
Ductility

ABSTRACT

In this paper, we show that there is a strong correlation between the strength differential (SD) effects in the plastic flow of the matrix, which arise from its dependence on the third stress invariant, void evolution, and ultimately the ductility of porous metallic polycrystals. For this purpose, detailed micromechanical finite-element analyses of three-dimensional unit cells are carried out. The plastic flow of the matrix is described by a criterion that accounts for strength-differential effects induced by shear deformation mechanisms of the constituent grains through a macroscopic parameter, k; only if there is no SD, k is zero, and the von Mises criterion is recovered. Numerical analyses are conducted for macroscopic proportional tensile loadings corresponding to fixed values of the stress triaxiality (ratio of the mean stress to the second stress invariant). It is shown that for the same macroscopic loading, the local plastic strains and the local stress distribution are strongly dependent on the sign of the parameter k. This in turn has a huge impact on damage accumulation, and ultimately affects the ductility of the porous polycrystals. Specifically, for axisymmetric loadings at third stress invariant positive, the rate of void growth is the slowest in the material with $\underline{k}$ negative, while the reverse holds true for equibiaxial tension (third stress invariant negative). Consequently, the ductility in axisymmetric tension at third-stress invariant positive is also markedly different from that in equibiaxial tension (third-stress invariant negative).

1. Introduction

Beginning with the pioneering studies of Needleman [1], Tvergaard [2], Koplik, and Needleman [3], micromechanical finite-element (FE) analyses of unit cells have been used to provide a better understanding of the mechanical response of porous solids (e.g., Richelsen and Tvergaard [4], Zhang et al. [5]; Srivastava and Needleman [6], etc.). In all these micromechanical studies, the plastic flow of the matrix (void-free material) is isotropic and is governed by the von Mises criterion.

However, early on it was recognized that the plastic flow of certain isotropic polycrystalline metallic materials is not governed by the von Mises criterion (e.g., Drucker [7]; the monograph of Prager and Hodge [8]; data reported by Lenhart [9] on pure copper; Billington [10] on iron; etc.). First, Hosford and Allen [11] demonstrated that strength differential

* Corresponding author. Tel.: +1 850 833 9350; fax: +1 850 833 9366.
E-mail address: cazacu@reef.ufl.edu (O. Cazacu).

http://dx.doi.org/10.1016/j.crme.2014.12.002
1631-0721/

(SD) effects whereby the compressive yield strength σ_C is different from the tensile yield strength σ_T arise in isotropic fully-dense face-centered cubic (FCC) and body-centered-cubic (BCC) polycrystals if deformation twinning is operational at the single-crystal level. Twinning being a shear deformation mechanism, these SD effects imply a dependence of the plastic flow of the polycrystal on the third invariant of the stress deviator (rather than say the mean stress, for more details see Cazacu and Barlat [12]). Concerning modeling of deformation twinning and its effects on the texture evolution of hexagonal close packed (HCP) polycrystals within the framework of crystal plasticity, the reader is referred to the seminal work of Van Houtte and collaborators, e.g., Van Houtte [13]; Leffers and Van Houtte [14]; Philippe et al. [15]; Coghe et al. [16]). As concerns very recent experimental studies devoted to the characterization of texture evolution in HCP polycrystals, see for example Khan et al. [17], Meredith and Khan [18].

In this paper we demonstrate that such SD effects of the plastic flow of the matrix have a significant influence on the porosity evolution and most importantly, the ductility of porous metallic polycrystals. To this end, a micromechanical study is conducted. It is assumed that the porous polycrystal contains a regular array of initially spherical voids. The matrix is considered to be elastic/plastic, the plastic flow being described by the isotropic form of the yield criterion of Cazacu et al. [19]. This yield criterion is pressure-insensitive, involves all principal values of the stress deviator, and a scalar material parameter, k, which accounts for SD effects.

The outline of the paper is as follows. After briefly reviewing the isotropic form of the criterion of Cazacu et al. [19], in Section 2 we present the micromechanical unit-cell model and the method used for the analysis. In Sections 3–4 are shown some results for three porous isotropic materials with a matrix characterized by different values of the parameter k, i.e. -0.3, 0, $+0.3$. For each porous polycrystal, the macroscopic loadings imposed are such that the principal values of the macroscopic stresses, Σ_1, Σ_2, Σ_3, follow a prescribed proportional loading history. Specifically, the dilatational response is investigated under axisymmetric loadings ($\Sigma_1 = \Sigma_2$) where the axial overall stress is adjusted so that a fixed ratio Σ_3/Σ_1 be maintained. Detailed analyses are presented for tensile loadings corresponding to ($\Sigma_1 = \Sigma_2$ and $\Sigma_3/\Sigma_1 = 2.5$) and equibiaxial tension ($\Sigma_1 = \Sigma_2$ and $\Sigma_3 = 0$), respectively. It is shown that for the same imposed macroscopic stress loading, the distribution of the local plastic strain and local stresses in the porous polycrystal is strongly influenced by the value of the macroscopic material parameter k, which accounts for the particularities of the plastic flow of the matrix. Moreover, a direct correlation is established between the sign of this macroscopic material parameter and the rate of void growth, which in turn affects all aspects of the macroscopic response of the porous polycrystal, most importantly its overall ductility.

2. Problem formulation and method of analysis

2.1. Yield criterion for the matrix

We consider that the void-free material is elastic–plastic, its yielding behavior being described by the isotropic form of the criterion of Cazacu et al. [19]. This criterion is expressed as:

$$\sqrt{\frac{9}{2(3k^2-2k+3)}\sum_{i=1}^{3}\left(|\sigma_i'|-k\sigma_i'\right)^2}=\sigma_T \tag{1}$$

where $\sigma_1', \sigma_2', \sigma_3'$ are the principal values of the deviator of the Cauchy stress tensor, $\boldsymbol{\sigma}' = \sigma - \sigma_m \mathbf{I}$; with $\sigma_m = \mathrm{tr}(\boldsymbol{\sigma})/3$ denoting the mean stress and $\mathbf{I}$ the second-order identity tensor, while σ_T is the yield stress in uniaxial tension. The only material parameter involved in the criterion is the parameter k, which is intimately linked with specific single-crystal plastic deformation mechanisms (e.g., see Lebensohn and Cazacu [20]). Its range of variation is $(-1, 1)$. If the constituent grains of a FCC polycrystal with uniform texture deform by $\{111\}\langle 110\rangle$ slip obeying Schmid law, plastic flow has no tension–compression asymmetry, i.e. the yield stress in uniaxial tension, σ_T, is the same as the yield stress in uniaxial compression, σ_C, the parameter k in Eq. (1) is zero and the isotropic form of the criterion of Cazacu et al. [19] reduces to the von Mises criterion. If twinning contributes to plastic deformation of the constituent grains, the polycrystal displays strength differential effects and $k \neq 0$, which means that the plastic flow depends on the sign and ordering of all principal values of $\boldsymbol{\sigma}'$ or alternatively on both invariants J_2 and J_3 of the stress deviator. For example, for a fully-dense isotropic FCC polycrystal that deforms at single-crystal level only by ($\{111\}\langle 112\rangle$) twinning (the usual conventions $\{\}$ and $\langle\rangle$, indicating respectively the twinning plane and direction types, are used), Hosford and Allen [11] showed that the plastic flow is pressure-insensitive, but the ratio between the yield stresses in uniaxial tension and compression is: $\sigma_T/\sigma_C = 0.83$, which corresponds to $k = -0.3$ (see Eq. (1)). On the other hand, for a fully-dense BCC polycrystal, for which the constituent grains deform solely by ($\{112\}\langle 111\rangle$) twinning the macroscopic yield stress in uniaxial tension is larger than in uniaxial compression, $\sigma_T/\sigma_C = 1.21$ (the reciprocal of the ratio for the FCC polycrystal), which according to the criterion given by Eq. (1) corresponds to $k = +0.3$ (minus the FCC value). Thus, the effect is just the opposite for BCC twinning in the easy direction. Note that these SD ratios reported by Hosford and Allen [11] represent a maximum obtained by assuming that all the twinning systems are able to twin in the easy direction. These results obtained with a Taylor-type crystal plasticity model were very recently confirmed by full-field calculations (see Lebensohn and Cazacu [20]). In Fig. 1a is shown the projection in the octahedral plane (plane normal to the hydrostatic axis, $\sigma_1 = \sigma_2 = \sigma_3$) of the yield criterion given by Eq. (1) for $k = -0.3$ in comparison with the von Mises

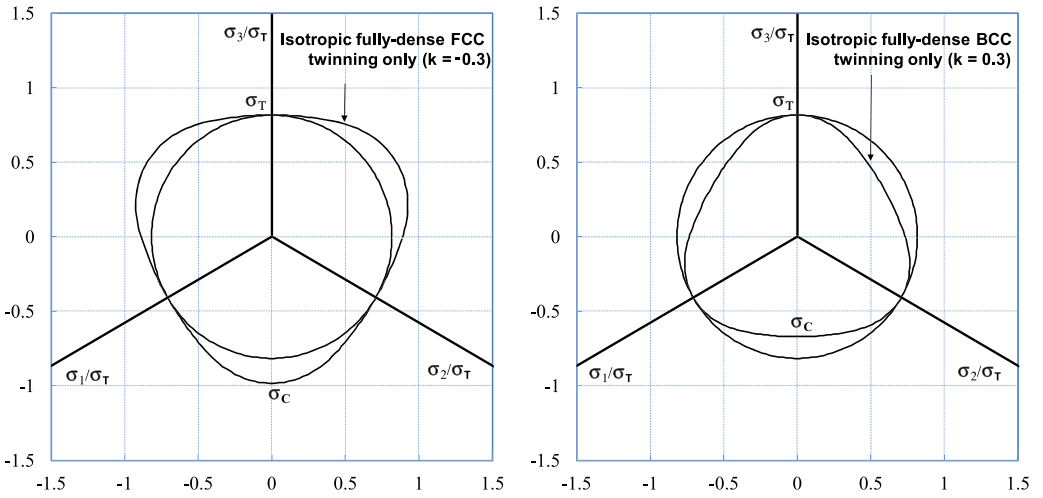

Fig. 1. (Color online.) Representation in the octahedral plane of the yield locus according to the isotropic form of Cazacu et al. [19] criterion (Eq. (1)) for fully-dense polycrystals with uniform texture deforming solely by twinning in comparison with the von Mises criterion ($k = 0$ in Eq. (1)): (a) FCC ($k = -0.3$) and (b) BCC polycrystals ($k = +0.3$).

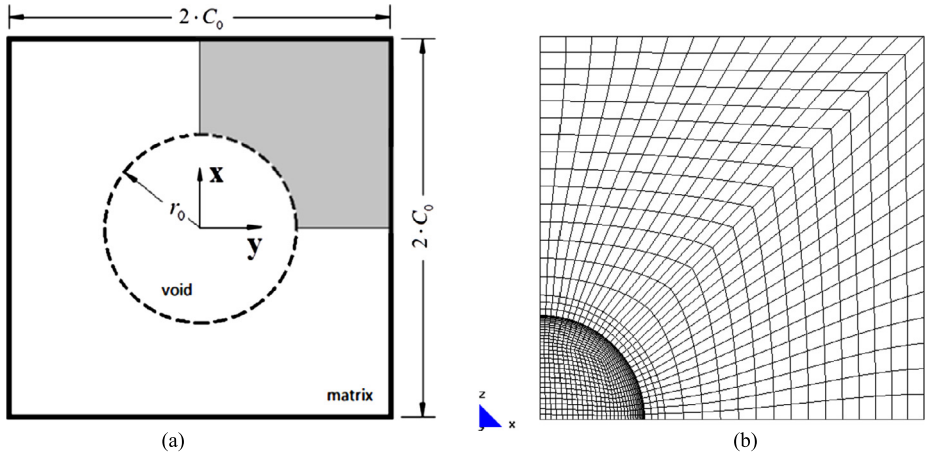

Fig. 2. (Color online.) (a) Schematic two-dimensional projection of the three-dimensional cubic cell model adopted in this study; $2C_0$ and r_0 denote the length of the undeformed cubic cell and the initial radius of the spherical void, respectively. (b) Finite-element mesh of one-eighth of the unit cell with a spherical void at its center.

yield criterion, which corresponds to $k = 0$ ($\sigma_T/\sigma_C = 1$), respectively; in Fig. 1b is shown the projection of the yield locus for the fully-dense BCC polycrystal ($k = +0.3$). Note the strong dependence of the yield loci on the third invariant of the stress deviator.

2.2. Unit-cell model

Full three-dimensional finite-element (FE) unit cell model computations are conducted. It is assumed that the porous polycrystal contains a regular array of initially spherical voids. The inter-void spacing is considered to be the same in any direction. Thus, the unit cell is initially cubic with side lengths $2C_0$ and contains a single void of radius r_0 at its center. The initial porosity is:

$$f_0 = \frac{\pi}{6}\left(\frac{r_0}{C_0}\right)^3 \tag{2}$$

The Cartesian tensor notation is used and the origin of the coordinate system is taken at the center of the void (see Fig. 2(a)). Let **u** denote the incremental displacement between the current and reference configuration, and **t** the prescribed Cauchy stress vector, defined on the current configuration. Symmetry conditions are imposed on the planes $x = 0$, $y = 0$, and $z = 0$, respectively:

$$u_1(0, y, z) = 0, \qquad t_2(0, y, z) = 0, \qquad t_3(0, y, z) = 0$$

$$u_2(x,0,z)=0, \qquad t_1(x,0,z)=0, \qquad t_3(x,0,z)=0$$
$$u_3(x,y,0)=0, \qquad t_1(x,y,0)=0, \qquad t_2(x,y,0)=0 \tag{3}$$

Therefore, only one-eighth of the unit cell needs to be analyzed numerically (see Fig. 2(b)). To simulate the constraints of the surrounding material, we enforce that the faces of the unit cell, which are initially planes parallel to the coordinate planes, remain planes and are shear-free. The boundary conditions imposed on the faces of the unit cell are:

$$u_1(C_0,y,z)=U_1^*(t), \qquad t_2(C_0,y,z)=t_3(C_0,y,z)=0$$
$$u_2(x,C_0,z)=U_2^*(t), \qquad t_1(x,C_0,z)=t_3(x,C_0,z)=0$$
$$u_3(x,y,C_0)=U_3^*(t), \qquad t_1(x,y,C_0)=t_2(x,y,C_0)=0 \tag{4}$$

The time histories of the displacements, $U_1^*(t)$, $U_2^*(t)$, and $U_3^*(t)$ in Eq. (4) are determined during the analysis in such a way that the overall Cauchy stresses Σ_1, Σ_2, Σ_3 follow a prescribed proportional loading history. The macroscopic true stresses Σ_1, Σ_2, Σ_3 are defined as:

$$\Sigma_1=\frac{1}{C_2C_3}\int_0^{C_2}\int_0^{C_3} t_1\,\mathrm{d}z\,\mathrm{d}y, \qquad \Sigma_2=\frac{1}{C_1C_3}\int_0^{C_3}\int_0^{C_1} t_2\,\mathrm{d}z\,\mathrm{d}x$$
$$\Sigma_3=\frac{1}{C_1C_2}\int_0^{C_1}\int_0^{C_2} t_3\,\mathrm{d}x\,\mathrm{d}y, \quad \text{where } C_i=C_0+U_i^* \tag{5}$$

are the current cell dimensions. The void is considered to be traction-free. For any given material, the strain paths imposed are such that the principal values of the macroscopic stresses, Σ_1, Σ_2, and Σ_3 follow a prescribed proportional loading history corresponding to either ($\Sigma_1=\Sigma_2$ and $\Sigma_3/\Sigma_1=2.5$) or equibiaxial tension (i.e. $\Sigma_1=\Sigma_2$ and $\Sigma_3=0$). The porous materials being isotropic, their mechanical response is fully characterized by the isotropic invariants of the overall stress, $\boldsymbol{\Sigma}$, i.e.:

$$\Sigma_{\mathrm{m}}=\frac{1}{3}(\Sigma_1+\Sigma_2+\Sigma_3); \qquad \Sigma_{\mathrm{e}}=\sqrt{3J_2^{\Sigma}}=\sqrt{\frac{3}{2}\left(\Sigma_1'^2+\Sigma_2'^2+\Sigma_3'^2\right)}; \qquad J_3^{\Sigma}=\Sigma_1'\Sigma_2'\Sigma_3' \tag{6}$$

where $\Sigma_i'=\Sigma_i-\Sigma_{\mathrm{m}}$, $i=1\ldots3$. The stress triaxiality ratio T_{Σ} is defined as the ratio between the first and second stress invariants, i.e. $T_{\Sigma}=\Sigma_{\mathrm{m}}/\sqrt{3J_2^{\Sigma}}$. The overall (macroscopic) principal strains, and the second-invariant of the macroscopic strain being calculated as follows:

$$E_1=\ln\left(\frac{C_1}{C_0}\right), \qquad E_2=\ln\left(\frac{C_2}{C_0}\right); \qquad E_3=\ln\left(\frac{C_3}{C_0}\right)$$
$$J_2^{\mathrm{E}}=\sqrt{\frac{1}{2}\left(E_1^2+E_2^2+E_3^2\right)}=\frac{\sqrt{3}}{2}E_{\mathrm{e}} \tag{7}$$

where C_0 and C_i, $i=1,\ldots,3$ are the initial and current cell dimensions and E_{e} is the macroscopic von Mises equivalent strain.

The void volume fraction, f, is evaluated at the end of each time increment as:

$$f=1-\frac{V_{\mathrm{matrix}}}{V_{\mathrm{cell}}}$$

In the above equation, $V_{\mathrm{cell}}=C_1C_2C_3$, where C_i denote the current dimensions of the cell, while the volume of the deformed matrix, V_{matrix}, is determined directly from the integration of the FE domain using the FE formulation ($V_{\mathrm{matrix}}=\sum_{i=1}^{N_{\mathrm{E}}} V_i$, where V_i is the volume of the element i and N_{E} is the total number of finite elements in the mesh).

The finite-element analyses were performed with DD3IMP [21,22], an in-house quasi-static elastoplastic code, using a fully-implicit time integration scheme FE solver. Fig. 2 shows the initial FE mesh of one-eighth of the unit cubic cell consisting of 12,150 elements (8-node hexahedral finite elements; selective reduced integration technique, with 8 and 1 Gauss points for the deviatoric and volumetric parts of the velocity field gradient, respectively) and a total of 13,699 nodes. A mesh refinement study was done to ensure that the results are mesh-independent.

In the FE implementation, special attention and care was paid so that all initially planar boundary surfaces remain strictly flat during the entire loading history. Specifically, the degrees of freedom of all FE nodes belonging to the same planar bounding surface of the cube were associated in the global stiffness matrix, and the equations of all these degrees of freedom were replaced by only one unknown variable.

Using the cell model, the mechanical response of porous isotropic materials with matrix characterized by: $k=-0.3$, $k=0$ (von Mises), and $k=0.3$. in Eq. (1) is investigated. The initial void volume fraction, $f_0=0.0104$ (which corresponds

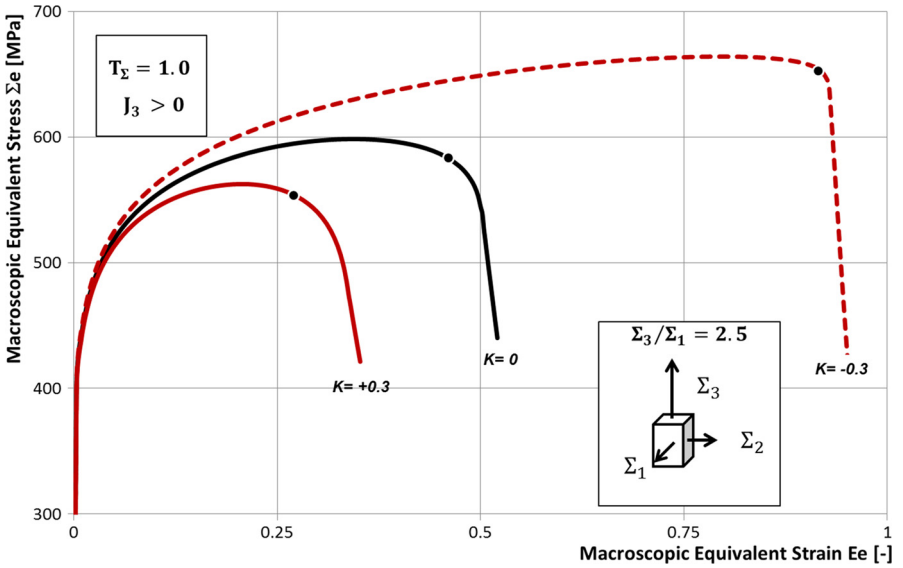

Fig. 3. (Color online.) Comparison between the macroscopic stress–strain response for porous materials with matrix displaying SD effects: $k = -0.3$, and $k = +0.3$ and von Mises behavior ($k = 0$), respectively for axisymmetric tensile loadings ($\Sigma_1 = \Sigma_2$ and $\Sigma_3/\Sigma_1 = 2.5$). Black dots mark the onset of failure.

to $r_0/C_0 = 0.271$) is considered to be the same in all materials. Thus, in the computations, only the material parameter k is varied. All the other input material parameters are kept the same, i.e. the elastic properties ($E = 200$ GPa, $\nu = 0.33$, where E is the Young modulus and ν is the Poisson coefficient) and the material parameters involved in the isotropic hardening law describing the evolution of the matrix tensile yield strength with local equivalent plastic strain, $\bar{\varepsilon}^{\mathrm{p}}$, i.e.

$$Y = A\left(\varepsilon_0 + \bar{\varepsilon}^{\mathrm{p}}\right)^n \tag{8}$$

where Y is the current matrix tensile flow stress, A, n and ε_0 are material parameters. The numerical values of these parameters are: $Y_0 = Y_{|\bar{\varepsilon}^{\mathrm{p}}=0} = 400$ MPa, $A = 881.53$ MPa, $n = 0.1$, $\varepsilon_0 = 0.00037$. It follows that all the differences in behavior between the porous materials are due solely to the specificities of the plastic flow of the matrix (SD effects), which are described by the macroscopic parameter k.

3. Mechanical response of the porous materials for axisymmetric tensile loading corresponding to $\Sigma_1 = \Sigma_2$ and $\Sigma_3/\Sigma_1 = 2.5$ ($J_3^{\Sigma} > 0$)

Using the micromechanical unit-cell model, we first examine the porosity evolution and its effects on the mechanical response of the porous materials for tensile loading corresponding to the following constant ratios between the principal stresses: $\Sigma_1 = \Sigma_2$ and $\Sigma_3/\Sigma_1 = 2.5$. This loading corresponds to a constant macroscopic stress triaxiality $T_\Sigma = 1$ (such level of triaxiality arises in tensile loading of blunt notched specimens, see also Tvergaard and Needleman [23]) and $J_3^{\Sigma} > 0$ during the entire loading history. Fig. 3 shows a comparison between the macroscopic effective stress vs. macroscopic effective strain (Σ_{e} vs. E_{e}) curves of the three porous materials; Fig. 4 shows the evolution of the void volume fraction, f, while Fig. 5 depicts the rate of void growth as a function of the macroscopic effective strain E_{e}. In each figure, and for each material, the onset of failure is marked by a black dot, while the final collapse is designated by an open circle. For all materials, the macroscopic strain E_{e} corresponding to the onset of failure is determined by monitoring the evolution of the cell's cross section that sustains the maximum applied load. For the macroscopic imposed loading, this is the cell's cross-section perpendicular to the axial axis Oz. For example, for the porous material with $k = +0.3$, in Fig. 6 is depicted the $\ln(C_0^2/C_1C_2)$ vs. E_{e} curve (solid curve), with C_i being the current values of the cell dimensions (see Eq. (5)) as well as the evolution of its first derivative i.e. $\delta\ln(C_0^2/C_1C_2)$ vs. E_{e} (interrupted line). The onset of failure corresponds to the strain at which there is an abrupt change in the slope of the $\delta\ln(C_0^2/C_1C_2)$ vs. E_{e} curve, while failure is considered to take place when the $\ln(C_0^2/C_1C_2)$ vs. E_{e} curve reaches a maximum, which corresponds to total loss of the load-carrying capacity (see also the discussion in Koplik and Needleman [3]). For each material, in Fig. 7 is highlighted the critical phase of the deformation process, where accelerated damage accumulation occurs (onset of failure to failure). It is clearly seen that all aspects of the mechanical response of the porous materials are influenced by the specificities of the plastic flow of the matrix. Specifically, the maximum effective stress that is reached, the onset of failure, and the maximum strain that is reached (which is a measure of the material's ductility) depend on the value of parameter k. Note that the porous material characterized by $k = -0.3$ has the highest ductility but the stress drop is also the most rapid (see the stress–strain curve of Fig. 3). This indicates that for this material the succession of events from onset of failure to final collapse is very fast (occurs within few percents of the macroscopic effective strain) and thus failure is more catastrophic than in a porous von

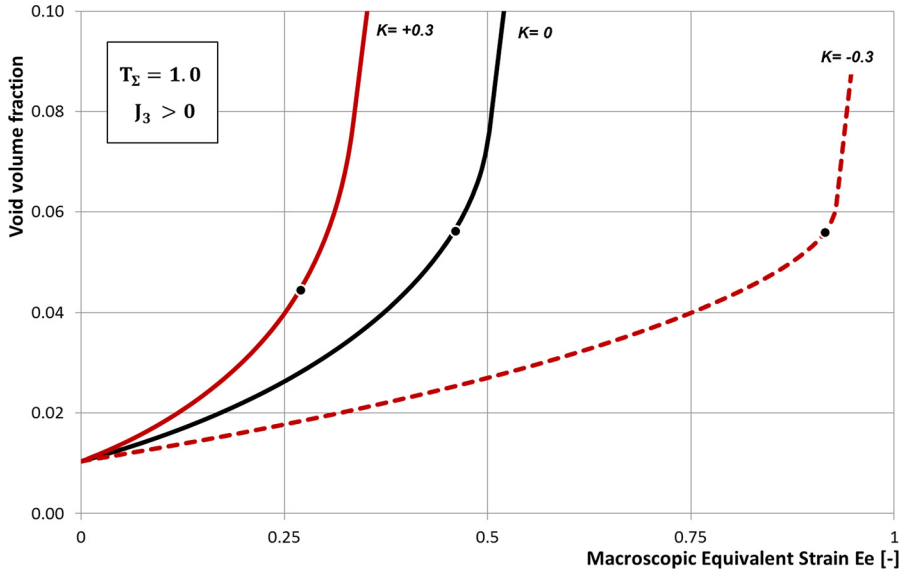

Fig. 4. (Color online.) Evolution of the void volume fraction with the macroscopic equivalent strain E_e, obtained by cell calculations for porous materials with matrix displaying SD effects: $k = -0.3$ and $k = +0.3$ and von Mises behavior ($k = 0$), respectively for axisymmetric tensile loadings ($\Sigma_1 = \Sigma_2$ and $\Sigma_3/\Sigma_1 = 2.5$). Black dots mark the onset of failure.

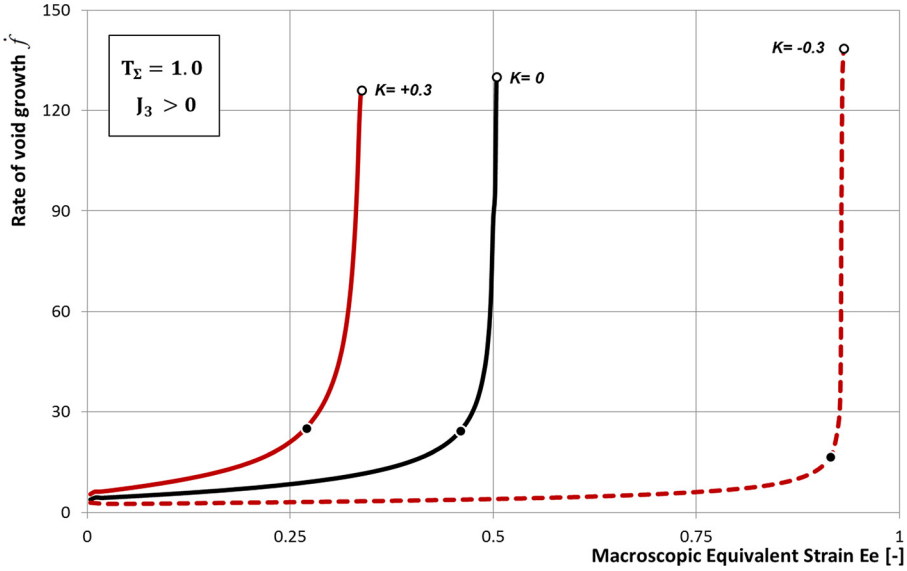

Fig. 5. (Color online.) Evolution of the void growth rate ($\dot{f}$) with the macroscopic equivalent strain E_e, obtained by cell calculations for voided polycrystals with matrix displaying SD effects: $k = -0.3$ and $k = +0.3 (\sigma_T/\sigma_C = 1.21)$ and von Mises behavior, respectively for axisymmetric tensile loadings ($\Sigma_1 = \Sigma_2$ and $\Sigma_3/\Sigma_1 = 2.5$). Black and white dots mark the onset of failure and total loss of load carrying capacity (collapse).

Mises material ($k = 0$) or in the porous material for which the plastic flow in the matrix is characterized by $k = 0.3$. The same conclusion can be drawn by examining the void volume fraction evolution (Fig. 4), the rate of void growth (Fig. 5), and the extent of the critical zone (depicted in Fig. 7). Indeed, for the material with $k = -0.3$ the rate of void growth is almost constant for most of the deformation process, i.e. until a macroscopic effective strain is reached when the rate of void growth increases very rapidly, indicating the onset of coalescence. Also, it is very worth noting that for this material the "critical zone" (from onset of failure to final collapse) is very limited, the macroscopic effective strain E_e corresponding to coalescence being very close to that at which final collapse occurs (see Fig. 7). In contrast, for the porous von Mises material and for the porous material characterized by $k = 0.3$, damage is more gradual. *The results presented highlight the difficulty in evaluating the life in service of metallic components, i.e. the value of the porosity* (*damage level*) *alone is not sufficient to estimate the safety of the structural parts.*

The paramount importance played by the plastic flow in the matrix on the ductility of the porous solids is clearly seen. For the porous material characterized by $k = -0.3$, the rate of void growth is significantly lower (see Fig. 4) than in the

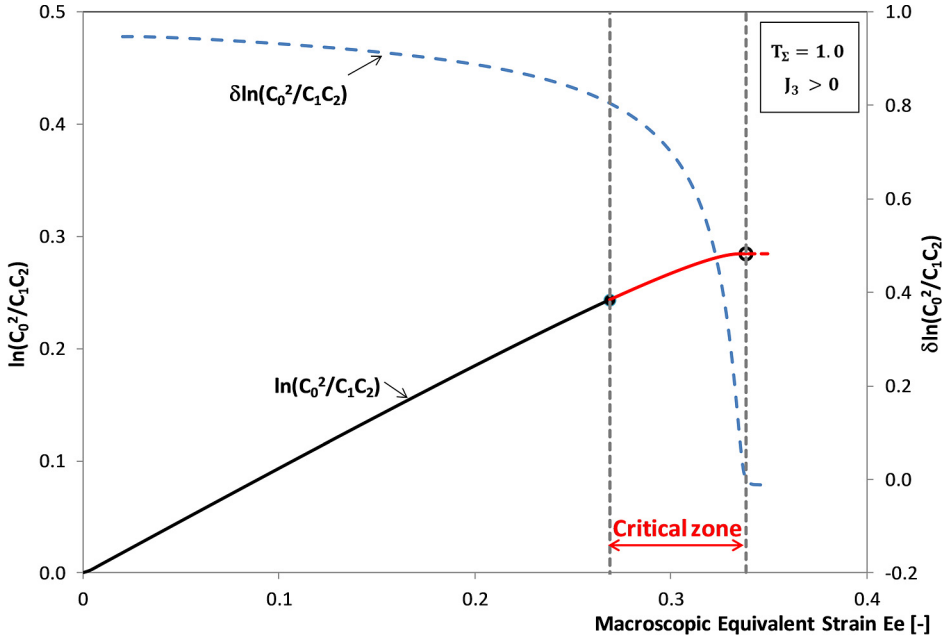

Fig. 6. (Color online.) Evolution of the load carrying cross-section with the macroscopic strain E_e (solid line) and $\delta \ln(C_0^2/C_1C_2)$ vs. E_e (interrupted line), respectively for the porous material with $k = +0.3$ for axisymmetric tensile loadings at $\Sigma_1 = \Sigma_2$ and $\Sigma_3/\Sigma_1 = 2.5$. The critical phase of the deformation process, where accelerated damage accumulation occurs (onset of coalescence to final collapse), is highlighted.

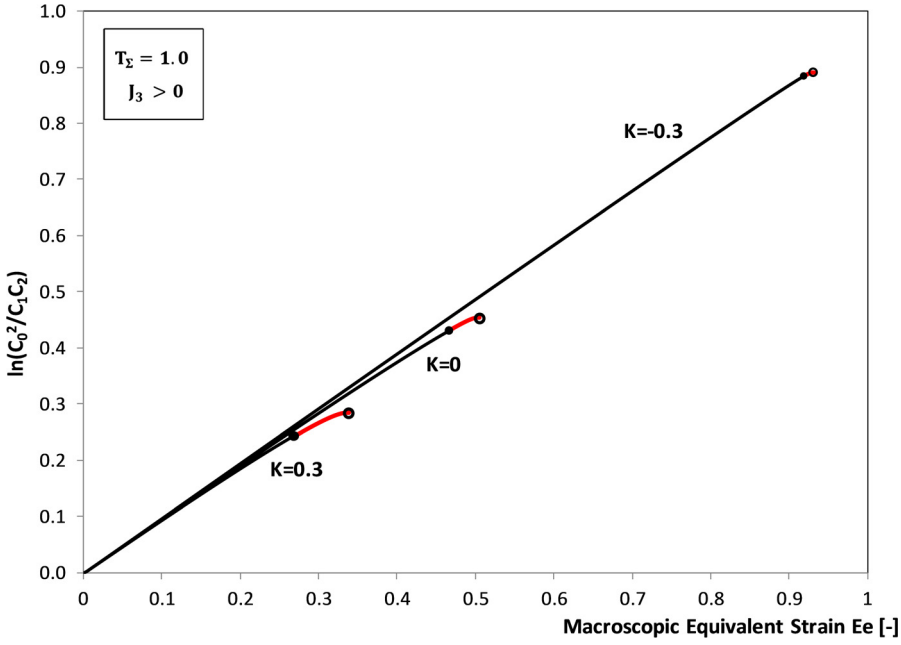

Fig. 7. (Color online.) Evolution of the load carrying cross-section with the macroscopic strain E_e for porous polycrystals with matrix displaying SD effects: $k = -0.3$ and $k = 0.3$ and von Mises behavior ($k = 0$), respectively for axisymmetric tensile loadings $\Sigma_1 = \Sigma_2$ and $\Sigma_3/\Sigma_1 = 2.5$. The dots mark the onset of void coalescence and total collapse, respectively.

other two materials, the macroscopic strain at the onset of failure being about three times higher than in a material with $k = 0.3$ (see Fig. 7). On the other hand, in the latter material ($k = 0.3$), the void growth is most rapid, which explains why this material exhibits the lowest ductility (see also Figs. 3–4).

To better understand the reasons for the very strong difference in void evolution between the three porous materials, we compare the local state fields corresponding to the same level of macroscopic true strain $E_e = 0.15$. Note that this strain level corresponds to the early stages of the deformation process where macroscopically only a very slight difference in the stress–strain response of the three materials can be observed (see Fig. 3). Fig. 8 shows the isocontours of constant local

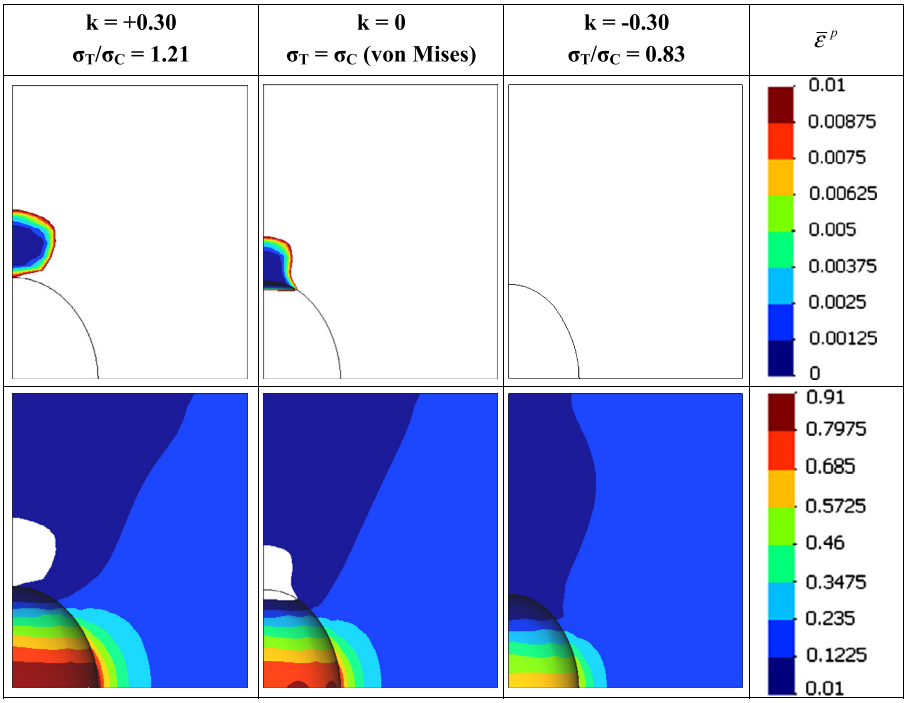

Fig. 8. (Color online.) Isocontours of the local effective equivalent plastic strain $\bar{\varepsilon}^{\mathrm{p}}$, corresponding to the same value of the macroscopic strain $E_{\mathrm{e}} = 0.15$ for the three porous materials for axisymmetric tensile loadings $\Sigma_1 = \Sigma_2$ and $\Sigma_3/\Sigma_1 = 2.5$. The upper figure corresponds to $0 \leq \bar{\varepsilon}^{\mathrm{p}} \leq 0.01$; the lower figure corresponds to $0.01 \leq \bar{\varepsilon}^{\mathrm{p}} \leq 0.91$. The white regions in the lower figure mark the elastic zones; only in the material with $k = -0.3$, the entire domain is plastic.

equivalent plastic strain, $\bar{\varepsilon}^{\mathrm{p}}$, corresponding to $E_{\mathrm{e}} = 0.15$. The local plastic strain $\bar{\varepsilon}^{\mathrm{p}}$ is the work-equivalent conjugate of the effective stress according to the criterion given by Eq. (1), i.e.

$$\dot{W}^{\mathrm{p}} = \dot{\bar{\varepsilon}}^{\mathrm{p}} \sqrt{\frac{9}{2(3k^2 - 2k + 3)} \sum_{i=1}^{3} \left(|\sigma_i'| - k\sigma_i'\right)^2} \tag{9}$$

Because of the drastic difference in the level of local plastic strains that develop in the three materials and in order to be able to better distinguish the distribution of the plastic zones while having the same scale (i.e. the same maximum and minimum levels for $\bar{\varepsilon}^{\mathrm{p}}$), for all materials, the upper Fig. 8 shows isocontours corresponding to $\bar{\varepsilon}^{\mathrm{p}} \leq 0.01$, while the lower Fig. 8 presents the isocontours corresponding to $0.01 \leq \bar{\varepsilon}^{\mathrm{p}} \leq 0.91$.

Examination of the upper part of Fig. 8 reveals that in the porous polycrystal characterized by $k = -0.3$ the entire domain (cell) has yielded. However, for the porous von Mises ($\sigma_{\mathrm{T}}/\sigma_{\mathrm{C}} = 1$) and the porous polycrystal characterized by $k = 0.3$, there exists a zone in the vicinity of the void along the vertical axis of the cross-section (Oz, which is the direction of the maximum applied load) where yielding did not occur. Specifically, for the porous von Mises material, the elastic zone is contiguous to the void, while for the material characterized by $k = 0.3$, the elastic zone is slightly shifted away from the void. Examination of the isocontours of local plastic strain for the range $0.01 \leq \bar{\varepsilon}^{\mathrm{p}} \leq 0.91$ show very marked differences in terms of the heterogeneity of plastic deformation and the distribution of the plastic zones within the cell. Note that for the porous polycrystal characterized by $k = -0.3$, the plastic deformation is more homogeneous than in the other materials. In contrast, at the same level of the macroscopic plastic strain $E_{\mathrm{e}} = 0.15$, in the von Mises material and in the polycrystal characterized by $k = 0.3$, the strain gradients along both the axial and transverse directions are much stronger. The highest levels of local plastic deformation and most heterogeneity are found in the material characterized by $k = +0.3$. A measure of the heterogeneity in plastic deformation within the domain is the ratio between the maximum local plastic strain in the entire domain, $\bar{\varepsilon}^{\mathrm{p}}_{\mathrm{max}}$, and the average of the local plastic strain, $\langle \bar{\varepsilon}^{\mathrm{p}} \rangle$ defined as:

$$\left\langle \bar{\varepsilon}^{\mathrm{p}} \right\rangle = \frac{1}{V} \int_{\mathrm{V}} \bar{\varepsilon}^{\mathrm{p}} \, \mathrm{d}V \tag{10}$$

Thus, the highest is the ratio $\frac{\bar{\varepsilon}^{\mathrm{p}}_{\mathrm{max}}}{\langle \bar{\varepsilon}^{\mathrm{p}} \rangle}$, the most heterogeneity there is. For the materials with $k = +0.3$, $k = 0$, and $k = -0.3$, these ratios are 5.95, 5.4, and 4.16, respectively. Note that the highest ratio (highest heterogeneity) is observed in the material with $k = +0.3$, while the lowest is in the material with $k = -0.3$.

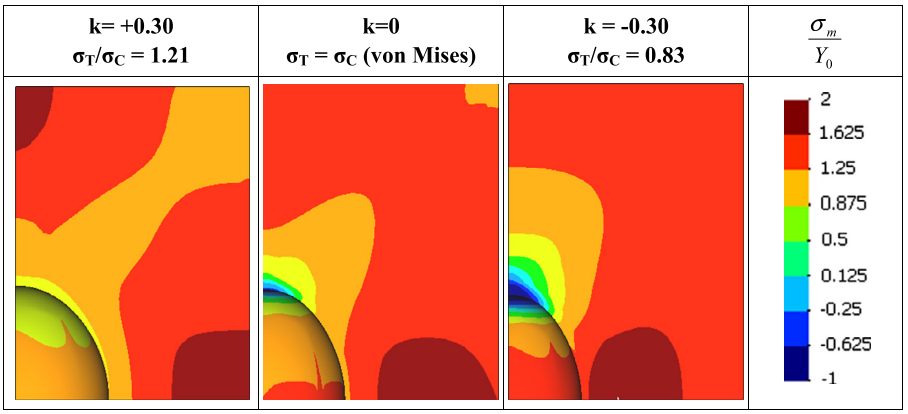

Fig. 9. (Color online.) Isocontours of the local normalized mean stress σ_m/Y_0 for the three porous polycrystals for axisymmetric tensile loadings $\Sigma_1 = \Sigma_2$ and $\Sigma_3/\Sigma_1 = 2.5$. Only for the material with $k = -0.3$ ($\sigma_T/\sigma_C = 0.83$), *an extended zone of negative (compressive) pressure contiguous to the void develops.*

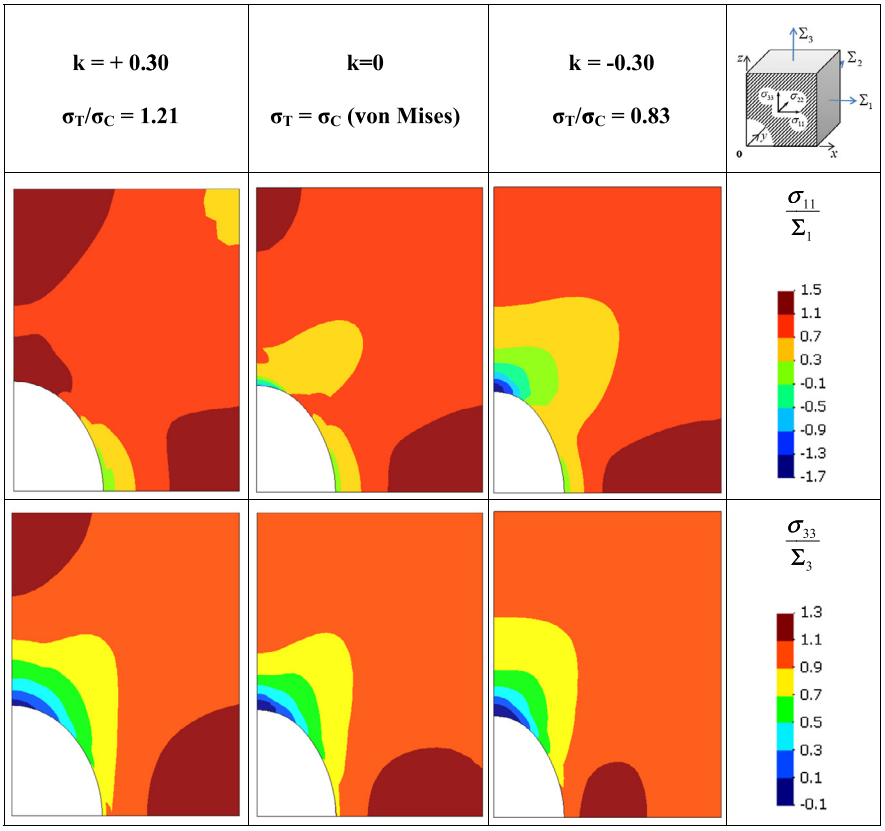

Fig. 10. (Color online.) Isocontours of the normalized local Cauchy stress components σ_{11} and σ_{22} for the three porous polycrystals for axisymmetric tensile loadings $\Sigma_1 = \Sigma_2$ and $\Sigma_3/\Sigma_1 = 2.5$.

Moreover, the distribution of the local stresses is markedly different depending on the value of k. Contours of constant mean stress σ_m/Y_0 are shown in Fig. 9. Note that in the material with $k = +0.3$ ($\sigma_T/\sigma_C = 1.21$), the local mean stress, σ_m/Y_0, is positive in the entire domain, while in the material with $k = -0.3$, which is fully plasticized, zones of negative mean stress develop near the void. As a consequence, for the latter material void growth is slowed down as compared to the material characterized by $k = +0.3$. This correlates with the differences in porosity evolution evidenced in Figs. 3–4.

To better understand why zones of negative mean stress develop only in the polycrystal with $k = -0.3$, in Fig. 10 are shown the isocontours of the components of the local Cauchy stress tensor σ_{11} and σ_{33} (normalized by the respective values of the macroscopic lateral stress Σ_1 and macroscopic axial stress, Σ_3, respectively). Note that only in the material with $k = -0.3$, the local lateral stress, σ_{11}, is negative (*compression*) in the vicinity of the void along the Oz direction

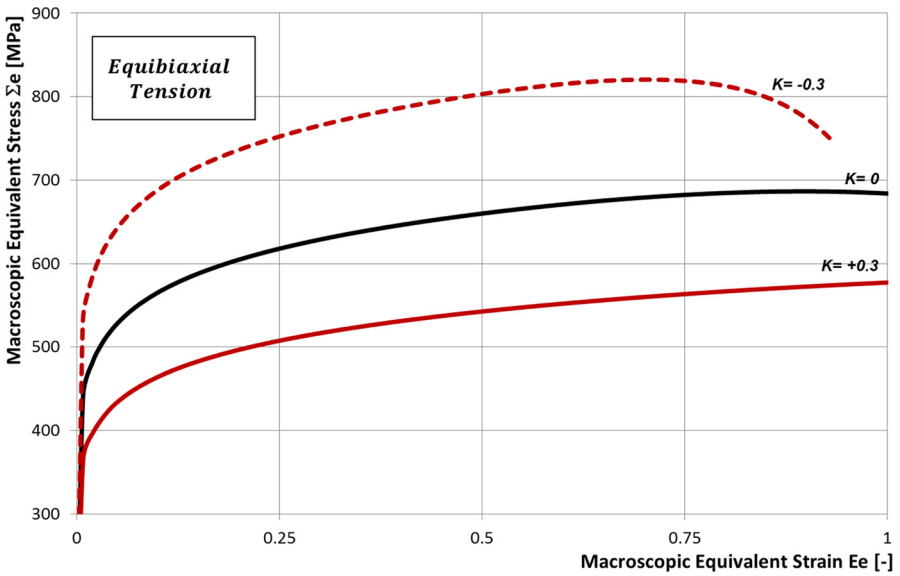

Fig. 11. (Color online.) Comparison between the macroscopic stress–strain response (equivalent stress Σ_e vs. macroscopic equivalent strain E_e) for porous polycrystals with matrix displaying SD effects: subjected to equibiaxial tensile loading ($\Sigma_1 = \Sigma_2$ and $\Sigma_3 = 0$; $J_3^{\Sigma} < 0$).

(direction of the maximum macroscopic loading direction), which results in negative values of the local mean stress, σ_m in the vicinity of the cavity.

In conclusion, although all materials were subjected to the same macroscopic tensile loading history corresponding to a constant macroscopic stress triaxiality $T_{\Sigma} = 1$ and $J_3^{\Sigma} > 0$ during the entire deformation process, the local fields are markedly different. *All the results presented highlight the strong correlation between the value of the macroscopic parameter k and the local plastic strain heterogeneity, which in turn leads to markedly different void evolution and ultimately ductility of the porous metallic materials* (see Figs. 3–4).

4. Mechanical response of the porous materials for equibiaxial tension ($\Sigma_1 = \Sigma_2 > 0$ and $\Sigma_3 = 0$)

Next, we examine the porosity evolution and its effects on the mechanical response of the three porous materials under equibiaxial tension, a loading of great practical importance in metal forming. Note that for such loading, $J_3^{\Sigma} < 0$ during the entire deformation process. Comparison between the macroscopic equivalent stress Σ_e vs. macroscopic equivalent strain E_e curves, obtained using the cell model for the three materials, is presented in Fig. 11. The evolution of the void volume fraction and the rate of void growth as a function of the macroscopic effective strain E_e are respectively shown in Figs. 12 and 13. Note that the specificities of the plastic flow of the matrix described by the parameter k affect every aspect of the mechanical response of the porous solid.

Under equibiaxial tension, only the material, which is characterized by $k = -0.3$ *displays softening; furthermore it has the lowest ductility. On the other hand, for this macroscopic stress path history, the von Mises material and the material characterized by* $k = +0.3$ *exhibit enhanced ductility* (*for these materials calculations were stopped at* $E_e = 1$). This correlates with the void volume fraction evolution (see Fig. 12) and the rate of void growth (Fig. 13) in each material. Indeed, under equibiaxial loading, in the material with $k = -0.3$ ($\sigma_T/\sigma_C = 0.83$) the void grows much faster than in the other materials and at some point in the deformation process, there is a very rapid increase in void volume fraction, which corresponds to the drop in the macroscopic effective stress (see Figs. 11–13). However, in the von Mises material ($k = 0$), the void grows much slower than in the material with $k = -0.3$, the rate of void growth being almost constant for most of the deformation process, while in the material with $k = 0.3$ there is a very little change in porosity for the entire process. To gain understanding of the differences in porosity evolution, we also examined the distribution of the local equivalent plastic strains (Fig. 14) and local stresses (Figs. 15–16) in each material corresponding to the same level of macroscopic effective strain $E_e = 0.5$. It is very worth noting that in the material where there is the least plastic heterogeneity, which is the material with $k = +0.3$, there is little damage accumulation (see also Figs. 12–13). For this material, the local stress distribution is more homogeneous (see Figs. 15–16), and the levels of mean stress σ_m/Y_0 are very low in most of the cell. In contrast, in the material with $k = -0.3$, the mean stress is much higher than in the others, the gradients of mean stress are much stronger and are due to the heterogeneity in the local stress component σ_{33}. Fig. 17 shows the evolution of the local strain heterogeneity ratio $\bar{\varepsilon}^p_{max}/\langle\bar{\varepsilon}^p\rangle$ vs. E_e for the three materials. Irrespective of the level of the macroscopic strain E_e, the local plastic strain heterogeneity is most pronounced in the material with $k = -0.3$, while in the material with $k = 0.3$ the local plastic strain is homogeneous for most of the deformation process.

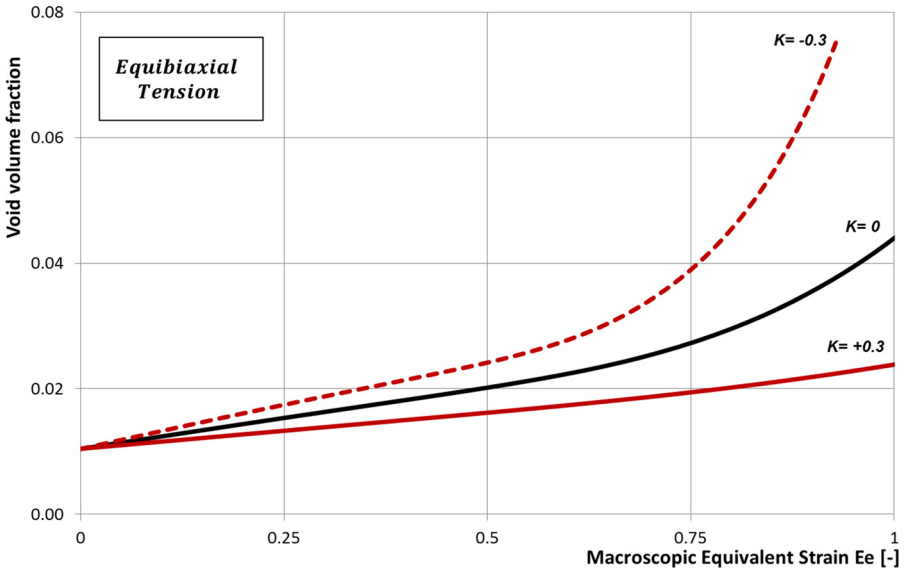

Fig. 12. (Color online.) Evolution of the void volume fraction with the macroscopic equivalent strain E_e, obtained by cell calculations for porous polycrystals matrix displaying SD effects: $k = -0.3$, $k = +0.3$, and von Mises behavior ($k = 0$), respectively, subjected to equibiaxial tensile loading.

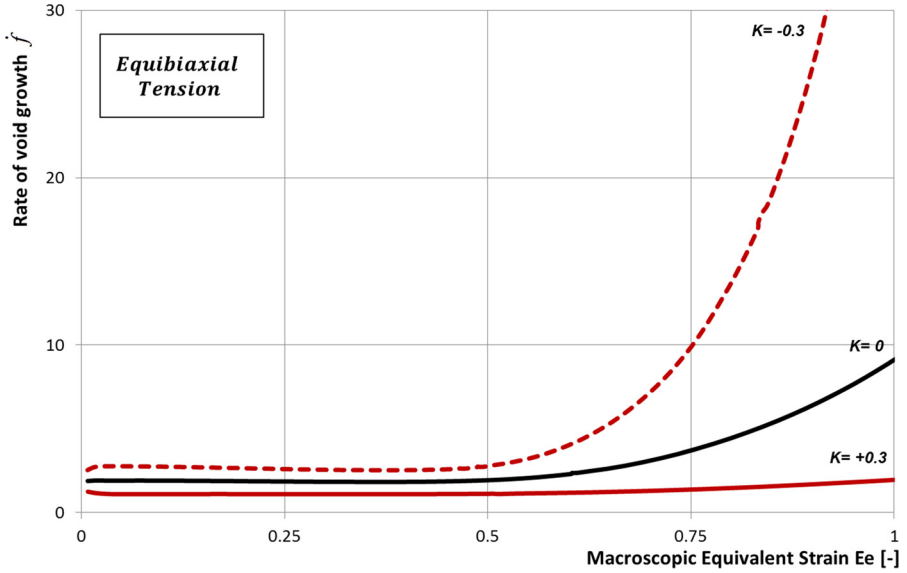

Fig. 13. (Color online.) Evolution of the void growth rate ($\dot{f}$) with the macroscopic equivalent strain E_e, obtained by cell calculations for porous polycrystals with matrix displaying SD effects: $k = -0.3$, $k = +0.3$, and von Mises behavior ($k = 0$), respectively, subjected to equibiaxial tensile loading. Note an almost constant and very low value of the rate of void growth for the material with $k = +0.3$.

5. Conclusions

In this paper, the SD effects in plastic flow of the matrix, which arise from the dependence of the plastic flow on the third invariant due to intrinsic single-crystal deformation mechanisms, on porosity evolution and the overall ductility of voided polycrystals was assessed for the first time. In doing this, a unit cell model for the porous media was used. Specifically, numerical analyses of three-dimensional unit cells were carried out for isotropic metallic polycrystals with constituent grains deforming solely by twinning. The twinning induced tension–compression asymmetry in the plastic flow at the polycrystal scale was modeled using the isotropic form of the yield criterion of Cazacu et al. [19]. This yield criterion is pressure-insensitive, it involves all principal values of the Cauchy stress deviator, and a scalar material parameter, k, which is intimately related to specific single-crystal plastic deformation mechanisms. For each porous polycrystal, the imposed macroscopic loadings were such that the principal values of the macroscopic stresses, Σ_1, Σ_2, Σ_3, followed a prescribed proportional loading history. Detailed analyses were presented for tensile axisymmetric loadings corresponding to ($\Sigma_1 = \Sigma_2$

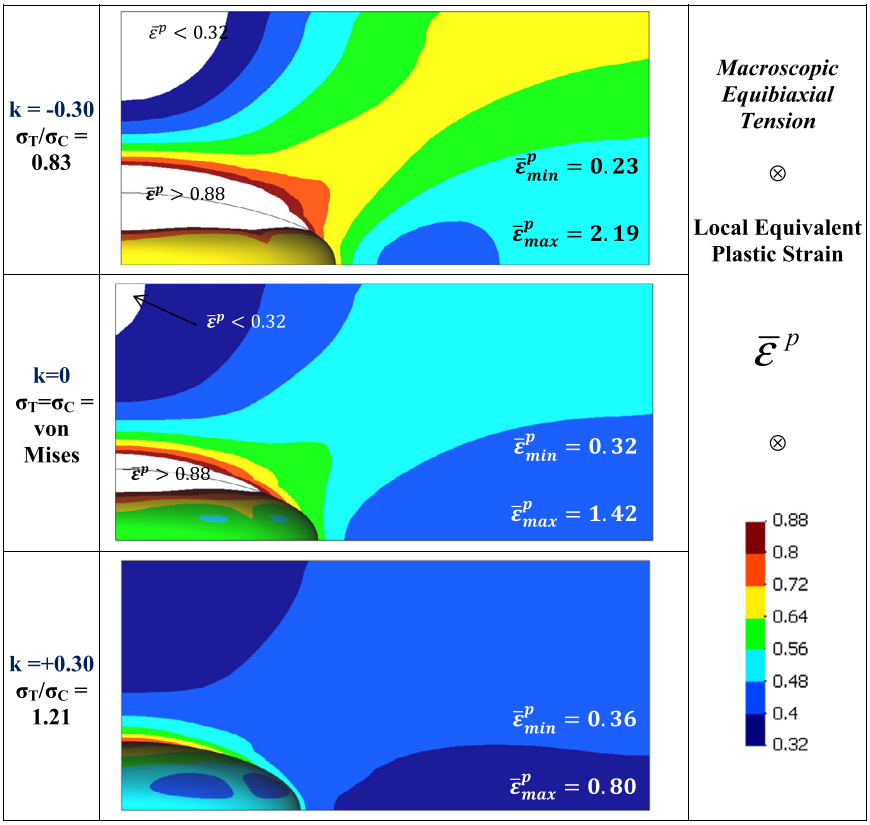

Fig. 14. (Color online.) Isocontours of the local effective equivalent plastic strain $\bar{\varepsilon}^{p}$ corresponding to the same value of the macroscopic strain $E_e = 0.5$: material with $k = -0.3$, von Mises material, and material with $k = +0.3$ subjected to equibiaxial tension. The white areas shown for the material with $k = -0.3$ and $k = 0$ represent either $\bar{\varepsilon}^{p} < 0.32$ or $\bar{\varepsilon}^{p} > 0.88$. The vertical axis is along the axial direction (no load), horizontal axis along the O*x* lateral direction.

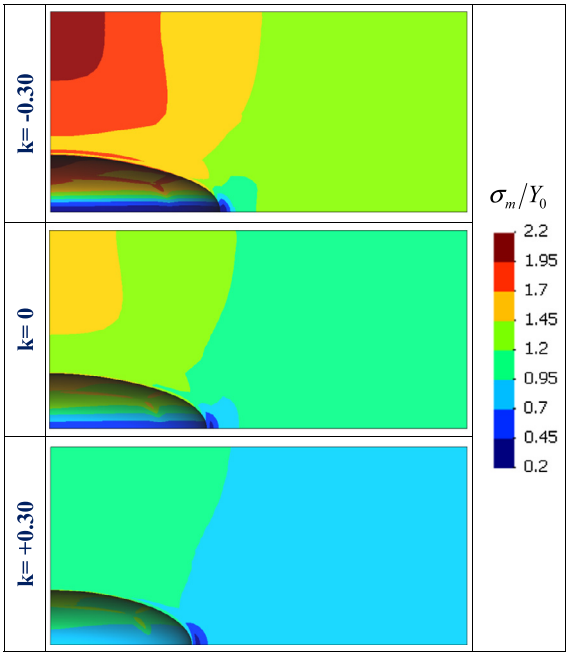

Fig. 15. (Color online.) Isocontours of the normalized local means stress σ_m/Y_0, corresponding to the same value of the macroscopic strain $E_e = 0.5$ for the three porous materials with $k = -0.3$, $k = +0.3$, and von Mises behavior ($k = 0$), respectively, subjected to equibiaxial tensile loading.

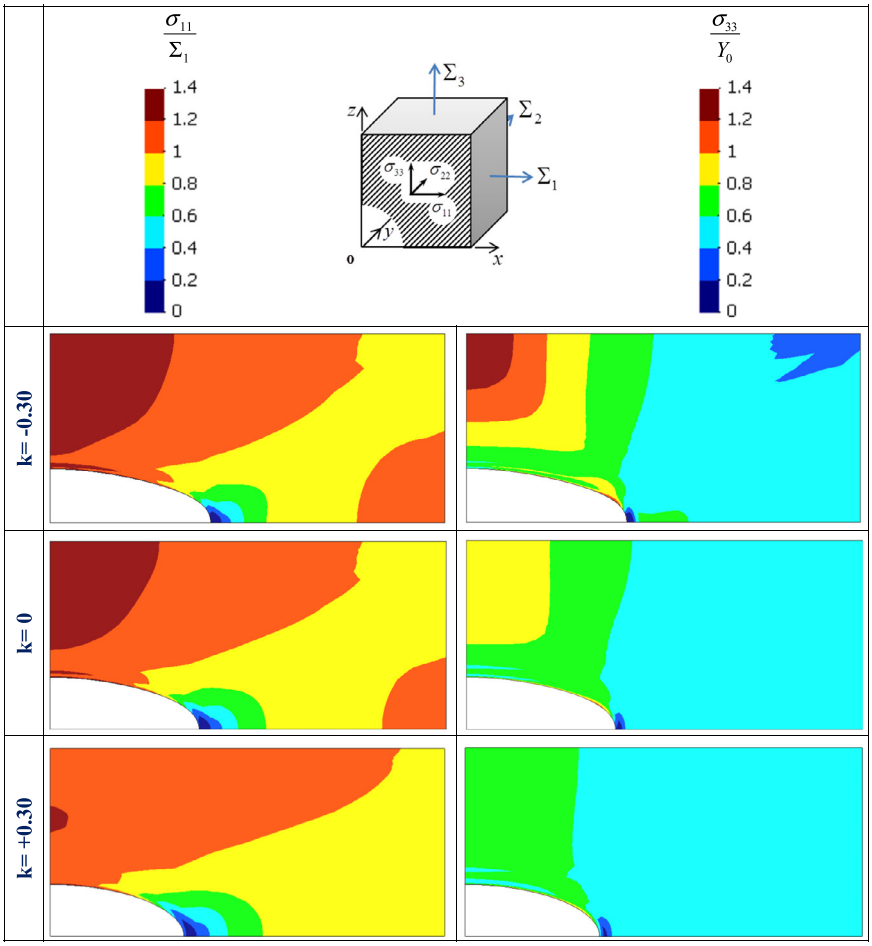

Fig. 16. (Color online.) Isocontours of the normalized local Cauchy stress components σ_{11}/Σ_1 and σ_{22}/Y_0, corresponding to the same value of the macroscopic strain $E_e = 0.5$ for the three porous materials with $k = -0.3$, $k = +0.3$, and von Mises behavior ($k = 0$), respectively, subjected to equibiaxial tensile loading (axial stress $\Sigma_3 = 0$).

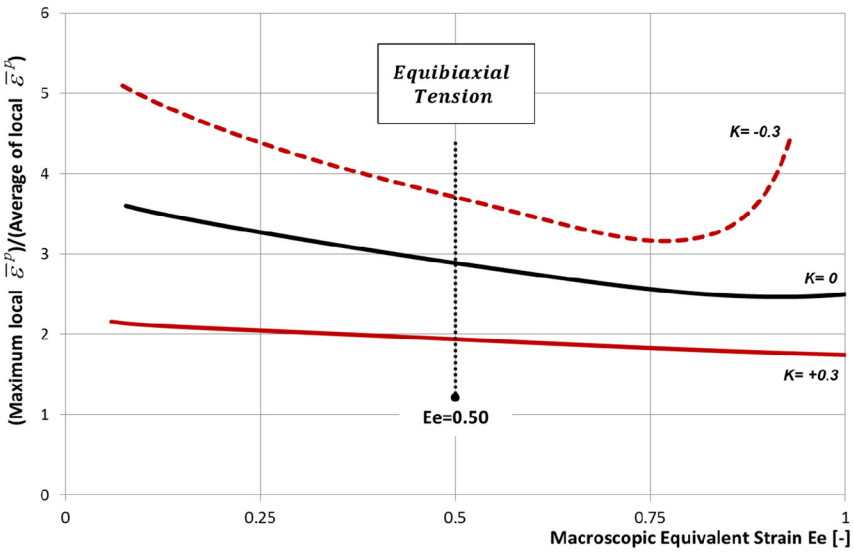

Fig. 17. (Color online.) Evolution of the local strain heterogeneity ratio $\bar{\varepsilon}^{\mathrm{p}}_{\max}/\langle\bar{\varepsilon}^{\mathrm{p}}\rangle$ with the macrocopic strain E_e for the three porous polycrystals subject to macroscopic equibiaxial tension; for each material $\bar{\varepsilon}^{\mathrm{p}}_{\max}$ is the maximum local plastic strain in the cell, and $\langle\bar{\varepsilon}^{\mathrm{p}}\rangle$ is the average of the local plastic strain in the cell.

and $\Sigma_3/\Sigma_1 = 2.5$) and equibiaxial tension ($\Sigma_1 = \Sigma_2$ and $\Sigma_3 = 0$), respectively. The first loading corresponds to axisymmetric tensile loading at $J_3^{\Sigma} > 0$ during the entire deformation process; the second loading corresponds to $J_3^{\Sigma} < 0$ for the entire deformation process.

It was clearly shown that irrespective of the imposed macroscopic loading, the tension–compression asymmetry in the plastic flow of the matrix, described by the parameter k, has a very strong influence on all aspects of the mechanical response of the porous materials.

For loading at *positive third stress invariant*, ($J_3^{\Sigma} > 0$) the porous material, which is characterized by $k = -0.3$ (yield in tension less than in compression) *has the highest ductility* (∼300% more than the material with $k = +0.3$—yield in tension larger than in compression), but the "critical zone" in the deformation process (onset of coalescence to failure) is very limited, the macroscopic effective strain E_e corresponding to coalescence being extremely close to that at which failure occurs (see Fig. 7). In contrast, for the porous von Mises material ($k = 0$) and for the porous material characterized by $k = 0.3$, damage is more gradual. *Moreover, it was shown that even if at the macroscopic level there is very little difference in the macroscopic stress–strain response between the porous polycrystals, the differences in the local state fields is very strong.*

However, for *equibiaxial tension* loadings, *which corresponds to negative third-stress invariant* ($J_3^{\Sigma} < 0$) *comparison between the rate of void growth and ductility in the same materials lead to completely different findings*: only the material, which is characterized by $k = -0.3$ (yield in tension less than in compression) displays softening; furthermore, it *has the lowest ductility*. The strong influence of the stress path history on plasticity–damage couplings is clearly evidenced. Specifically, for loadings such that $J_3^{\Sigma} > 0$, the fastest void growth rate occurs in the material characterized by $k = +0.3$; on the other hand, for loadings such that $J_3^{\Sigma} < 0$, the fastest void growth rate occurs in the material characterized by $k = -0.3$. Thus, this study indicates a direct correlation between a macroscopic material parameter that is intimately related to the particularities of the plastic flow (i.e. the parameter k describing the SD ratio of the matrix) and the rate of void growth for a given strain path.

While in the examples shown here the tension–compression asymmetry of the polycrystalline materials was induced by twinning at the single-crystal level, this strength differential at the polycrystal level may arise from other single-crystal plasticity mechanisms, e.g., when different components of the applied stress affect the single crystal plastic deformation by climb and glide [24].

References

[1] A. Needleman, Void growth in an elastic–plastic medium, J. Appl. Mech. 39 (1972) 964–969.
[2] V. Tvergaard, Influence of voids on shear band instabilities under plane strain conditions, Int. J. Fract. 17 (1981) 389–407.
[3] J. Koplik, A. Needleman, Void growth and coalescence in porous plastic solids, Int. J. Solids Struct. 24 (8) (1988) 835–853.
[4] A.B. Richelsen, V. Tvergaard, Dilatant plasticity or upper bound estimates for porous ductile solids, Acta Metall. Mater. 42 (1994) 2561–2577.
[5] K.S. Zhang, J.B. Bai, D. Francois, Numerical analysis of the influence of the Lode parameter on void growth, Int. J. Solids Struct. 38 (2001) 5847–5856.
[6] A. Srivastava, A. Needleman, Porosity evolution in a creeping single crystal, Model. Simul. Mater. Sci. Eng. 20 (2012) 1–23.
[7] D. Drucker, Relation of experiments to mathematical theories of plasticity, J. Appl. Mech. 16 (1949) 349–357.
[8] W. Prager, P. Hodge, Theory of Perfectly Plastic Solids, John Wiley & Sons, Inc., 1951.
[9] R.E. Lenhart, The relationship of hardness measurements to the tensile and compression flow curves, WADC technical report 55-114, General Electric Research Laboratory, 1955.
[10] E. Billington, Non-linear mechanical response of various metals: I dynamic and static response to simple compression, tension and torsion in the as received and annealed states, J. Phys. D 10 (1977) 519–531.
[11] W.F. Hosford, T.J. Allen, Twining and directional slip as a cause for strength differential effect, Metall. Trans. 4 (1973) 1424–1425.
[12] O. Cazacu, F. Barlat, A criterion for description of anisotropy and yield differential effects in pressure-insensitive materials, Int. J. Plast. 22 (2004) 2027–2045.
[13] P. Van Houtte, Simulation of the rolling and shear texture of brass by the Taylor theory adapted for mechanical twinning, Acta Metall. 26 (1978) 591–604.
[14] T. Leffers, P. Van Houtte, Calculated and experimental orientation distributions of twin lamellae in rolled brass, Acta Metall. 37 (1989) 1191–1198.
[15] M.J. Philippe, M. Serghat, P. Van Houtte, C. Esling, Modelling of texture evolution for materials of hexagonal symmetry—II. Application to zirconium and titanium α or near α alloys, Acta Metall. Mater. 43 (1995) 1619–1630.
[16] F. Coghe, W. Tirry, L. Rabet, D. Schryvers, P. Van Houtte, Importance of twinning in static and dynamic compression of a Ti–6Al–4V titanium alloy with an equiaxed microstructure, Mater. Sci. Eng. A 537 (2012) 1–10.
[17] A. Khan, A. Pandey, T. Gnaupel-Herold, R.K. Mishra, Mechanical response and texture evolution of AZ31 alloy at large strains for different strain rates and temperatures, Int. J. Plast. 27 (2011) 688–706.
[18] C.S. Meredith, A.S. Khan, Texture evolution and anisotropy in the thermo-mechanical response of UFG Ti processed via equal channel angular pressing, Int. J. Plast. 30–31 (2012) 202–217.
[19] O. Cazacu, B. Plunkett, F. Barlat, Orthotropic yield criterion for hexagonal closed packed materials, Int. J. Plast. 22 (2006) 1171–1194.
[20] R.A. Lebensohn, O. Cazacu, Effect of single-crystal plastic deformation mechanisms on the dilatational plastic response of porous polycrystals, Int. J. Solids Struct. 49 (2012) 3838–3852.
[21] L.F. Menezes, C. Teodosiu, Three-dimensional numerical simulation of the deep-drawing process using solid finite element, J. Mater. Process. Technol. 97 (2000) 100–106.
[22] M.C. Oliveira, J.L. Alves, L.F. Menezes, Algorithms and strategies for treatment of large deformation frictional contact in the numerical simulation of deep drawing process, Arch. Comput. Methods Eng. 15 (2008) 113–162.
[23] V. Tvergaard, A. Needleman, Analysis of the cup-cone fracture in a round tensile bar, Acta Metall. 32 (1984) 157–169.
[24] R.A. Lebensohn, C.S. Hartley, C.N. Tomé, O. Castelnau, Modelling the mechanical response of polycrystals deforming by climb and glide, Philos. Mag. 90 (2010) 567–583.